Title: Shared PRAME Epitopes are T-Cell Targets in NUT Carcinoma

Running Title: PRAME in NUT Carcinoma

Authors: Jeffrey L. Jensen[††1,2], Sara K. Peterson[††2,3], Shawn Yu[1,2], Tomoaki Kinjo[2,4], Brandon A. Price[5], Maria Sambade[2], Steven P. Vesko[2], Johnathan D. DeBetta[6], Julie K. Geyer[2,7], Kwangok P. Nickel[8], Randall J. Kimple[8,9], Rishi S. Kotecha[10,11,12], Laura E. Herring[2], Ian J. Davis[2,13], Jeremy R. Wang[2,7], Christopher A. French[14], Brian Kuhlman[2,4], Alex Rubinsteyn[xx2,3], Jared Weiss[xx1,2], Benjamin G. Vincent[*xx15,16]

[††] = co-first authorship

[xx] = co-last authorship

* = corresponding author

Corresponding Author

Benjamin G. Vincent, MD

Associate Professor of Medicine, Division of Hematology

Joint Faculty, Department of Microbiology and Immunology

Curriculum in Bioinformatics and Computational Biology

Computational Medicine Program
Lineberger Comprehensive Cancer Center
University of North Carolina at Chapel Hill
5206 Marsico Hall, Chapel Hill, NC 27599
Benjamin_Vincent@med.unc.edu, @BenjaminGVincen

1: Division of Medical Oncology, Department of Medicine, The University of North Carolina at Chapel Hill, Chapel Hill, North Carolina

2: Lineberger Comprehensive Cancer Center, Chapel Hill, North Carolina

3: Department of Genetics, Curriculum in Bioinformatics and Computational Biology, The University of North Carolina at Chapel Hill, Chapel Hill, North Carolina

4: Department of Biochemistry and Biophysics, University of North Carolina at Chapel Hill, Chapel Hill, North Carolina

5: Tempus AI, Inc., Chicago Illinois

6: Department of Biochemistry and Molecular Biology, John Hopkins Bloomberg School of Public Health, Baltimore, Maryland

7: Department of Pathology and Laboratory Medicine, University of North Carolina at Chapel Hill, Chapel Hill, North Carolina

8: Department of Human Oncology, University of Wisconsin School of Medicine and Public Health, University of Wisconsin, Madison, WI

9: University of Wisconsin Carbone Cancer Center, University of Wisconsin School of Medicine and Public Health, University of Wisconsin, Madison, WI

10: Department of Clinical Haematology, Oncology, Blood and Marrow Transplantation, Perth Children's Hospital, Perth, Austrailia

11: Leukaemia Translational Research Laboratory, WA Kids Cancer Centre, The Kids Research Institute Austrailia, University of Western Austrailia, Perth, Austrailia

12: Curtin Medical School, Curtin University, Perth, Austrailia

13: Division of Hematology-Oncology, Department of Pediatrics, The University of North Carolina at Chapel Hill, Chapel Hill, North Carolina

14: Department of Pathology, Brigham and Women's Hospital, Harvard Medical School, Boston, Massachusetts

15: Division of Hematology, Department of Medicine, The University of North Carolina at Chapel Hill, Chapel Hill, North Carolina

16: Department of Microbiology and Immunology, The University of North Carolina at Chapel Hill, Chapel Hill, North Carolina

Keywords: NUT carcinoma, PRAME, T-Cell Receptor Bispecifics, Cancer-specific Antigens, Brenetafusp, IMC-F106C, BRD4::NUTM1, BRD3::NUTM1, NSD3::NUTM1

Declarations:

Ethics approval and consent to participate: All genetic engineering experiments involving lentivirus or siRNAs were approved by the UNC Institutional Biosafety Committee. All animal experiments were approved by the UNC Institutional Animal Care and Use Committee. All patient samples analyzed in the Tempus AI Sequencing Database were deidentified, and patients consented for their deidentified data to be used in research.

Consent for publication: All authors consent that contingent on the acceptance thereof, for this research to be published in JITC with all appropriate requirements of copyright and access as this journal demands.

Availability of data and material: Gene expression data from all sequencing will be deposited in GEO. Mass spectrometry raw data and all other raw data will be made available upon request to the corresponding author.

Competing interests: The authors declare no competing interests.

Funding: JLJ was supported by a Conquer Cancer Young Investigator Award, paid for by the New Rhein Foundation. Any opinions, findings, and conclusions expressed in this material are those of the author(s) and do not necessarily reflect those of the American Society of Clinical Oncology®, Conquer Cancer®, or the New Rhein Foundation. JLJ was supported additionally by a Lung Cancer Initiative Fellowship Award, the UNC Department of Medicine Core Facilities CFAC Award, as well as the IM-TAG T32. RJK was supported by P50CA278595, R37 CA255330, and P30 CA014520. This work was also supported by The Max Vincze Foundation (AR and BGV), The Victor Family Foundation (AR and BGV), philanthropic support from the Ben Brown Family (JW), and

the NIH grant R35GM131923. IJD is supported by the V Foundation for Cancer Research and the NIH (R01-CA276663).

Authors' contributions:

JLJ – Hypothesis generation, performed experimentation for all figures, wrote the first draft of the manuscript, and obtained funding

SKP – Hypothesis generation, performed sequencing analysis, and wrote the first draft of the manuscript

SY – Designed and produced αPRAME$_{425}$ x SP34 αCD3 bispecific, performed testing in T2 cells and NSCLC cells, and edited manuscript

TK - Designed and produced αPRAME$_{425}$ x SP34 αCD3 bispecific, performed testing in T2 cells and NSCLC cells, and edited manuscript

BAP – Curated the *NUTM1* fusion cohort in the Tempus AI Sequencing Database and performed sequencing analysis

MS – Produced western blots and samples for immunopeptidomics

SV – Produced data from LENS and the corresponding figures, and also wrote the methods section for LENS

JDD – Prepared samples for western blotting and immunopeptidomics

JKG – Analyzed long read DNA sequencing

KPN – Prepared and provided the NUT carcinoma patient-derived xenograft

RJK - Prepared and provided the NUT carcinoma patient-derived xenograft

RSK – Prepared and provided the NUT carcinoma cell line JCM1

LEH - Analyzed immunopeptidomics data and generated mass spectrum figures. Reviewed and revised mass spectrometry methods section.

IJD – Mentored SKP, assisted in sequencing analysis, and revised the manuscript

JRW – Mentored JKG and analyzed long read DNA sequencing

CAF – Provided NUT carcinoma cell lines, produced NUT carcinoma tissue microarray and stained it for PRAME, and revised the manuscript

BK – Mentored SY and TK, designed and produced αPRAME425 x SP34 αCD3 bispecific, and revised the manuscript

AR – Mentored SKP, hypothesis generation, analyzed sequencing data, obtained funding and revised the manuscript

JW – Mentored JLJ, hypothesis generation, revised the manuscript, and obtained funding

BGV – Mentored JLJ, hypothesis generation, revised the manuscript, and obtained funding

Acknowledgments: We would like to acknowledge the work and contributions from multiple core facilities at UNC including the Immune Monitoring and Genomics Facility (IMGF), the High Throughput Sequencing Facility (HTSF), and the lentiviral/shRNA core facility.

List of Abbreviations:

Landscape of Neoantigen Software (“LENS”)

Non-small cell lung cancer (“NSCLC”)

T-cell receptor (“TCR”)

Cancer testis antigen (“CTA”)

Bispecific T-cell engager (BiTE)

Immune mobilizing monoclonal T-cell receptors against cancer (ImmTAC)

Dulbecco’s Modified Eagle Medium (DMEM)

Patient-derived xenograft (PDX)

Transcripts per million (TPM)

Relative centrifugal force (RCF)

Abstract (Words=297, Word Limit=350. 401 words counting accessories):

Background: NUT carcinoma is a rare but highly lethal solid tumor without an effective standard of care. NUT carcinoma is caused by bromodomain-containing *NUTM1* fusion oncogenes, most commonly *BRD4::NUTM1*. BRD4::NUTM1 recruits p300 to acetylate H3K27 forming expansive stretches of hyperacetylated chromatin called “megadomains” with the overexpression of encapsulated oncogenes, including *MYC*. We hypothesized that transcriptional dysregulation caused by BRD4::NUTM1 would lead to the generation of cancer-specific antigens that could be therapeutically actionable.

Methods: We integrated genomics, immunopeptidomics, computational antigen prediction software, and gain/loss-of-function genetic experiments on a panel of cell lines (N=5), a patient derived xenograft, a tissue microarray (N=77), and on patient samples from the Tempus AI Sequencing Database harboring evidence of *NUTM1* fusions (N=165). We also created an αPRAME$_{425}$ T-cell receptor x SP34 αCD3 bispecific molecule modeled after the clinically tested IMC-F106C αPRAME$_{425}$ T-cell receptor bispecific T-cell engager, and we applied this to NUT carcinoma cells *in vitro*.

Results: We identified *PRAME* as the most commonly expressed cancer/testis antigen in patient samples harboring the three canonical NUT carcinoma fusions (*BRD4::NUTM1*, *BRD3::NUTM1*, and *NSD3::NUTM1*). Additionally, 56% (43/77) of NUT carcinoma tissue microarray samples stained positive for PRAME. Immunopeptidomics detected more PRAME-derived HLA ligands (N=9) than all other cancer/testis antigens combined (N=5). *BRD4::NUTM1* expression in HEK 293T cells enhanced PRAME levels and *BRD4::NUTM1* knockout in NUT carcinoma cells reduced PRAME levels. The αPRAME$_{425}$ T-cell receptor x SP34 αCD3 bispecific molecule exhibited potent, T-cell mediated cytotoxicity against *PRAME*+ but not *PRAME*- NUT carcinoma cells *in vitro*.

Conclusions: PRAME is highly expressed in NUT carcinoma and the most common oncoprotein causing NUT carcinoma, BRD4::NUTM1, contributes to these high PRAME levels. PRAME epitopes presented by HLA Class I are a previously unrecognized therapeutic vulnerability for NUT carcinoma that warrant clinical trials testing PRAME targeted immunotherapies in this neglected patient population.

What is already known on this topic: NUT carcinoma is a devastating malignancy that is recalcitrant to cytotoxic chemotherapy, T-cell checkpoint blockade, and targeted therapies in the form of bromodomain inhibitors.

What this study adds: NUT carcinoma tumors are high in the cancer/testis gene *PRAME*. The oncogene most commonly causing NUT carcinoma, *BRD4::NUTM1*, contributes to these high levels. NUT carcinoma cells present PRAME epitopes on HLA Class I molecules and are susceptible to PRAME-directed, T-cell mediated cytotoxicity.

How this study might affect research, practice or policy: Our results argue for phase I/II clinical trials testing PRAME immunotherapies like IMC-F106C in *PRAME*+ NUT carcinoma patients.

Graphical Abstract:

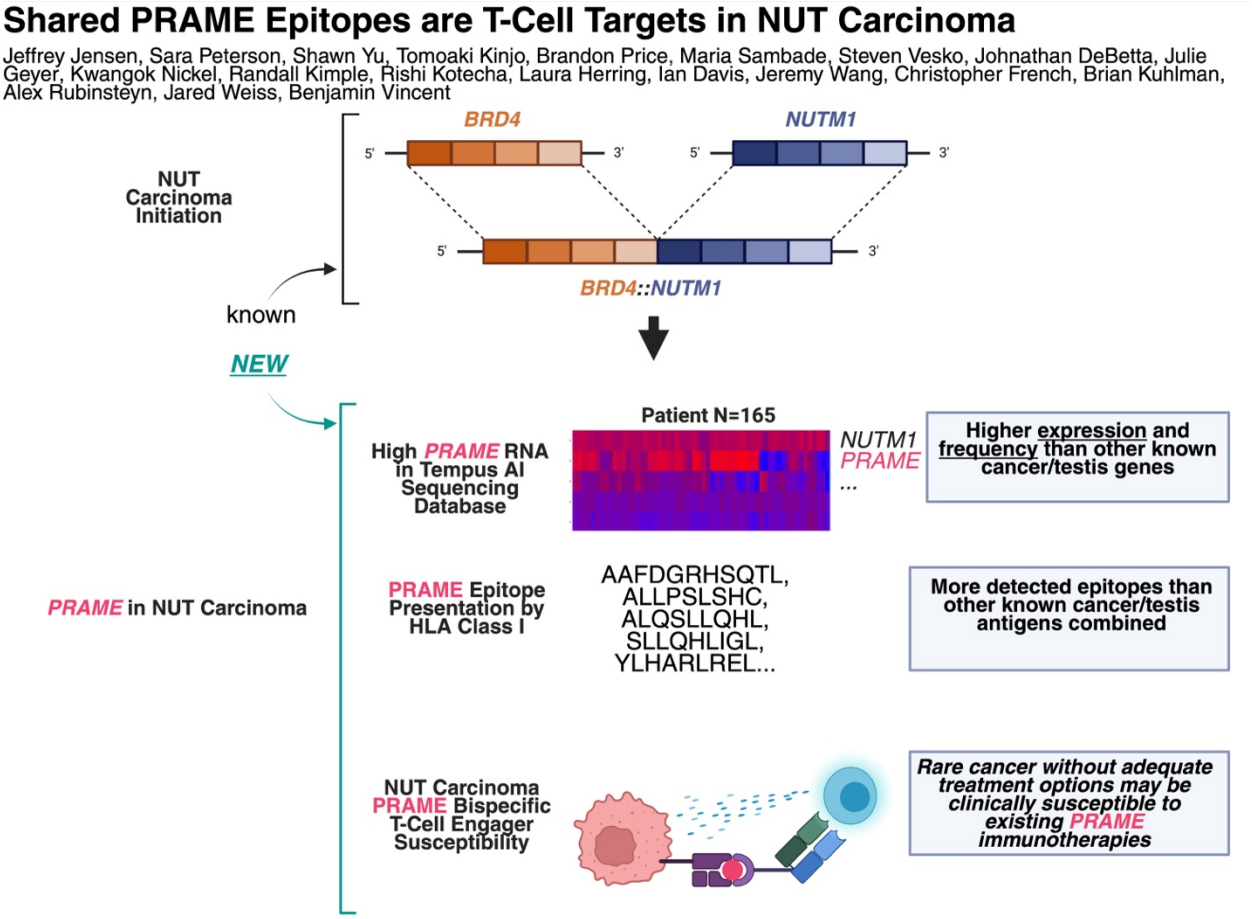

Background (Words = 633):

NUT carcinoma is a rare but underdiagnosed and devastating malignancy defined by ectopic expression of the Nuclear Protein in Testis gene ("*NUT*" or "*NUTM1*"), most commonly through an in-frame translocation to the bromodomain-containing *BRD4* with formation of the *BRD4::NUTM1* fusion gene (75% of cases) (1). BRD4::NUTM1 is a potent oncoprotein that initiates NUT carcinoma by binding to acetylated H3K27 ("H3K27ac"), recruiting p300 and catalyzing the hyperacetylation of adjacent histones resulting in extended hyperacetylated domains ("megadomains") with the corresponding overexpression of oncogenes, including *MYC* and *SOX2* (2, 3). NUT carcinoma was formerly labeled as NUT Midline Carcinoma owing to a predilection for afflicting midline

structures and is now known to occur most commonly in the lungs and sinonasal passages (4). NUT carcinoma is not associated with smoking or any known exposures and afflicts individuals of all ages including infants, children, and young adults (5-7). Clinical outcomes in adults are dismal with median survival after diagnosis of 6.7 months and similar outcomes in children (4, 8). Treatment for localized disease is focused on aggressive attempts at local control with wide local resection and adjuvant radiation and/or chemotherapy, but even among NUT carcinoma patients treated with surgery first outcomes are poor. In one cohort, surgery first patients experienced a median survival time of 415 days post-diagnosis with no patient surviving for more than 3 years post diagnosis (4, 9).

Therapeutics research to date has focused on blocking the binding of BRD4 to H3K27ac using bromodomain inhibitors, but in phase I/II clinical trials bromodomain inhibitors have yielded progression free survival times of only 1-2 months (10-13). At the time of this writing, all clinical trials testing new therapeutics for NUT carcinoma patients in the United States are testing bromodomain inhibitors (NCT05019716, NCT05372640, and NCT05488548). NUT carcinoma tumors are PD-L1 low, tumor mutational burden low, and immune “cold” tumors that are also highly refractory to cytotoxic chemotherapy and T-cell checkpoint blockade (4). New treatment modalities are clearly needed.

Interest in treating challenging solid tumors with HLA-restricted TCR-based therapies is growing. The first phase III clinical trial of a TCR x CD3 activator bispecific (also known

as an ImmTAC) showed overall survival benefit in the frontline setting for HLA A02+ uveal melanoma targeting the gp100 peptide (14). Recently, the SPEARHEAD-1 trial showed durable responses in patients with heavily pre-treated synovial sarcoma or myxoid round cell liposarcoma with afamitresgene autoleucel: a TCR T-cell therapy expressing a TCR targeting an HLA-A02 bound epitope from the cancer/testis gene *MAGEA4* (15). This resulted in the first TCR T-cell product approval for afamitresgene autoleucel and was quickly followed up by the IGNYTE-ESO trial which similarly showed durable responses in the same disease types with letetresgene autoleucel: another TCR T-cell product targeting epitopes from the cancer/testis gene *NY-ESO-1* (HLA A*02:01, A*02:05, or A*02:06) (16).

Like NUT carcinoma, both synovial sarcoma and myxoid/round cell liposarcoma are uncommon fusion protein-driven malignancies. For each of these sarcomas, >90% of cases harbor the pathognomonic t(X;18) or t(12;16)(q13;p11), respectively (17, 18). Whereas MAGEA4 and NY-ESO-1 antigens are common in these sarcomas, the antigenic landscape of NUT carcinoma and the susceptibility of NUT carcinoma to T-cell mediated therapeutics are unknown. We hypothesized that if BRD4::NUTM1 causes dysregulated gene transcription through reliable epigenetic changes, then BRD4::NUTM1 could also upregulate genes encoding cancer specific antigens that would serve as actionable TCR targets. Here we show that BRD4::NUTM1 causes transcription of the cancer/testis gene *PRAME*, and that *PRAME* is the predominant cancer/testis gene expressed within a clinical patient cohort of *NUTM1* fusion genes and especially in patients with canonical NUT carcinoma fusions (*BRD4::NUTM1*,

BRD3::NUTM1, *NSD3::NUTM1*) (19). We also show that NUT carcinoma cells present PRAME epitopes with HLA Class I and are susceptible to T-cell mediated killing mediated by an affinity-matured PRAME epitope TCR x CD3 activating bispecific molecule. Our work identifies PRAME as a promising target for cancer vaccines, TCR-based therapies, and TCR-mimetics in NUT carcinoma phase I/II clinical trials.

Methods (Words = 1,652):

Reagents

Cell lines were maintained in DMEM with 10% FBS and penicillin/streptomycin. The PDX was propagated in the flanks of NSG mice with Matrigel and purified using tumor dissociation and mouse cell depletion kits (Miltenyi Biotec). RNA was isolated using RNEasy columns (Qiagen). Western blots used PVDF and blocking in 5% milk. Antibodies are described in **Supplementary Table 1**. siRNA transfections were performed with Lipofectamine RNAiMAX and 10 µM pools of four siRNAs synthesized by IDT with [dT][dT] overhang, desalted purification, and no 3' modifications (**Supplementary Table 2**). Tet-on, blasticidin selection lentiviral pInducer20 vectors containing *BRD4::NUTM1* or *GFP* have been described (20). VSV-G pseudotyped lentiviral particles were packaged in 293T cells and purified by filtration. Tissue microarray immunohistochemistry was done by BWH Dana-Farber-Harvard Medical School Specialized Histopathology Services-Longwood (SHL) Core using αPRAME (Biocare Medical ACI3252B, 1:100).

Immunopeptidome Predictions

Antigen prediction used LENS v1.2-dev. Sample-level FASTQs were trimmed and filtered for quality using FASTP 0.23.1. The resulting FASTQ pairs were aligned to a modified hg38 reference genome (excluding the Epstein-Barr Virus (EBV) contig) using STAR 2.7.0f with parameters *--quantMode TranscriptomeSAM --outSAMtype BAM SortedByCoordinate --twopassMode Basic --outSAMunmappedWithin*. Transcript-level quantifications were generated using Salmon 1.1.0 with a GENCODE v37 GTF, augmented with human retroviral-like sequences from gEVE. CTAs were defined using a manually curated list of genes with testis and placenta-specific expression (**Supplementary Table 3**). The initial list of CTAs was pulled from CTDatabase and manually filtered using Human Protein Atlas.

Splice variants were detected using NeoSplice. Expressed viruses were detecting using the VirDetect workflow. HLA typing for class I alleles was performed using seq2HLA 2.2. We processed protein sequences from CTAs in the 95th expression percentile for downstream peptide prediction. Gene fusions were predicted using STARfusion 1.10.1 with recommended parameters and trimmed RNA FASTQs. Relevant protein sequences derived from CTAs, fusion, splice variants, viruses, and ERVs were filtered for potential peptides of interest using NetMHCpan 4.1b.

Bispecific Protein Production

Coding sequences for PRAME soluble TCR specific for the HLA-A*02:01-restricted SLLQHLIGL epitope were derived from sequences previously described for the PRAME

Vα and Vβ domains and from the Protein Data Bank ID 6U07 crystal structure for the computationally thermostabilized Cα and Cβ domains (21, 22). Chimeric SP-34 αCD3 heavy and light chain sequences were published previously (23). One primary fusion construct and two auxiliary constructs were generated as clonal genes in mammalian expression vector plasmids (Twist Bioscience). The primary fusion constructs consisted of the SP-34 αCD3 heavy chain, a $(Gly_4Ser)_4$ linker, PRAME TCR Vα/Cα, and an 8xHis-Tag. The first auxiliary coding sequence encoded for SP-34 αCD3 light chain; the second for PRAME TCR Vβ/Cβ (**Supplementary Table 4)**.

All three plasmid constructs were co-transfected for transient expression in Expi293F cells cultured with Expi293 Expression Medium at 50 mL scale using ExpiFectamine 293 Transfection Kit, similarly to previously described with the following modifications (24). Plasmids for primary fusion construct, first auxiliary construct, and second auxiliary construct were mixed in a 3:1:1 mass ratio, totaling 1 µg plasmid mixture per milliliter of cell culture. At 18 hours after transfection, enhancer 1 (300 µL at 50 mL scale) and enhancer 2 (3 mL at 50 mL scale) and 6 mL of 3.5% (w/v) Hyclone Cell Boost 1 were added to the cells. Cell culture supernatant was harvested at 96 hours after transfection by pelleting cells at 3428 RCF at 4°C for 15 min and further clarified using a 0.22 µm polyvinylidene difluoride membrane filter (Millipore). Assembled PRAME bispecific constructs were affinity purified by batch-binding clarified medium with pre-equilibrated penta-Ni resin (Marvelgent) for 1 hour at 4° C and then transferred into a column to collect the resin. A three-step wash was performed by gravity at room temperature (RT) to eliminate protein contaminants. The first wash was performed with 6 CV (column volume) of high-salt Tris buffer [50 mM Tris (pH 8.0) and 1 M sodium chloride with 10

mM imidazole]; the second was performed with 2 CV wash with 1× PBS (pH 7.4) with 20 mM imidazole; and the third was performed with 2 CV wash with 1× PBS (pH 7.4) with 40 mM imidazole. Bound proteins were eluted in one step using 5 CV of 1× PBS (pH 7.4) and 500 mM imidazole to collect the protein and then sequential concentration at 4°C using a 30K MWCO Amicon-4 followed by an Amicon-0.5 centrifugal filter at maximum allowed RCF for each filter, serially exchanged into 1× PBS (pH 7.4) to ensure at least 1:1000 dilution of imidazole. Purity was assessed by SDS-polyacrylamide gel electrophoresis.

Cytotoxicity Assays

Whole blood was obtained from Gulf Coast Regional Blood Center. Peripheral blood monocytes were isolated using Ammonium-Chloride-Potassium Lysing Buffer and Density Gradient Medium (Stemcell Technologies). T-cells were isolated using a negative selection, magnetic bead kit (Stemcell Technologies) and then incubated with RPMI and 10% FBS for 5 days in an αCD3 coated (5 µg/mL, BD Biosciences) flask with carrier-free IL-2 (2 ng/mL, R&D Systems) and αCD28 (2.5 µg/mL, BD Biosciences). Expanded T-cells were co-cultured in RPMI media with 10% FBS. Luminescence output was either read using CellTiter-Glo 2.0 reagent for luciferase-free cell lines or by adding luciferin (250 µg/mL, Promega). Peptide pulses used 1 µg/mL of SLLQHLIGL peptide, synthesized by the UNC High-Throughput Peptide Synthesis and Array Facility, over three hours.

RNA Sequencing

Library preparation used Illumina's Stranded mRNA Prep Ligation kit, starting with 125 ng of RNA. The average fragment length for these libraries was between 300-400 bp. Paired-end sequencing was performed using the NovaSeq 6000 version 1.5 (2X100), obtaining at least 45M reads per sample. Bulk RNA-seq samples were processed using selected components of the nf-core RNA-seq pipeline (v3.14), an open-source workflow managed with Nextflow. Reads were demultiplexed, and quality was assessed using FastQC, with results summarized in MultiQC. Adapter trimming was performed with cutadapt, ribosomal RNA was removed with SortMeRNA, followed by alignment to the GRCh38 reference genome using STAR. Transcript-level quantification was conducted with Salmon. Counts were summarized to the gene level and normalized to TPM to generate a gene x sample matrix. All downstream visualization and analysis were performed in R. All scripts used for this project are publicly available on GitHub (https://github.com/pirl-unc/PRAME_in_NUT_Carcinoma).

Immunopeptidomics

Snap frozen cell pellets were submitted to Biognosys for immunopeptidomics. Samples and a processing quality control sample (JY cells) were lysed using Biognosys' Lysis Buffer for 1 hour at 4° C. After removal of cell debris, the lysates were incubated with bead coupled antibodies (clone W6/32) to capture HLA class I complexes with associated peptides. Bound protein complexes were washed and peptides eluted using Biognosys' optimized immunopeptidomics protocol. Clean up for mass spectrometry

was carried out using an Oasis HLB µElution Plate (30 µm). Immunopeptides were dried down using a SpeedVac system and resuspended in 10 ul of 1% acetonitrile and 0.1% formic acid in water. Samples were pooled and fractionated into 5 fractions using high pH reversed phase fractionation (HPRP) for spectral library generation.

For DDA LC-MS/MS measurements of fractionated samples, 8 µl of immunopeptides per sample were injected to a Biognosys in-house packed reversed-phase column on a NeoVanquish UHPLC nano liquid chromatography system connected to a Orbitrap Exploris 480 mass spectrometer equipped with a Nanospray Flex ion source and a FAIMS Pro ion mobility device. LC solvents were A: water with 0.1% FA, B: 80% acetonitrile. The nonlinear LC gradient was 1 - 40% solvent B in 120 minutes followed by a column washing step in 90% B for 11 minutes, and a final equilibration step of 1% B for 5 minutes at 64° C with a flow rate set to 250 nl /min. MS1 precursor scans were acquired between 330-1250 m/z at 120,000 resolution with data dependent MS2 scans at 60,000 resolution. MS2 scans were acquired in cycle time of 1.6 s and 1.4 s per applied FAIMS compensation voltage. Only precursors with charge state 1-5 were isolated for dependent MS2 scans.

For DIA LC-MS/MS measurements of study samples, 8 µl of immunopeptides per sample were injected to a Biognosys in house packed reversed phase column on a NeoVanquish UHPLC nano liquid chromatography system connected to a Orbitrap Exploris 480 mass spectrometer equipped with a Nanospray Flex ion source and a FAIMS Pro ion mobility device (Thermo Scientific). The system was used in trap and elute configuration using a 300 µm x 5 mm PepMap Neo C 18 Trap 3 PK cartridge pre column (Thermo Scientific 174502). LC solvents were A: water with 0.1% FA, B: 80%

acetonitrile, 0.1% FA in water. The nonlinear LC gradient was 1-40% solvent B in 120 minutes followed by a column washing step in 90% B for 11 minutes, and a final equilibration step of 1% B for 5 minutes at 64° C with a flow rate set to 250 nl /min. The FAIMS DIA method consisted of one full range MS1 scan and 20 DIA segments as adopted from Bruderer et al (25) and Tognetti et al (26).

The shotgun and HRM mass spectrometric data was analyzed using Spectronaut v18, the false discovery rate on peptide and protein level was set to 1 %. A human UniProt .fasta database (Homo sapiens, 2025-01-01) appended with *NUTM1* fusion proteins was used for the search engine, also supplemented with mutated *NUTM1* and *PRAME* isoform fastas, allowing for non-specifically digested peptides (no trypsin cleaved termini) with a length between 7 and 12 amino acids, max. 2 variable modifications (N-term acetylation, carbamidomethylation [C], pSTY) and requiring carbamidomethylation methionine oxidation as fixed modification. The identification results were then exported as a hybrid spectral library. Raw HRM mass spectrometric data were analyzed using Spectronaut v18 with Qvalue filtering and no background signal integration or imputation. The hybrid spectral library generated in this study was used. Peptide level false discovery rate control was 1 % and cross-run normalization using global normalization to the median. MS2 spectra were visualized and annotated using the Interactive Peptide Spectral Annotator. Fragment ion tolerance was set to 5ppm for a-, b-, and y-ions.

Results (Words=1,546):

RNA sequencing and computational predictions suggest PRAME and NUTM1 are sources of HLA Class I peptide ligands in NUT carcinoma

To test the hypothesis that transcriptional dysregulation due to NUTM1 fusion oncoproteins would lead to the production of cancer-specific antigens, we obtained five NUT carcinoma cell lines (TC-797, 10-15, 14169, PER403, and JCM1) and one patient derived xenograft ("PDX") described in **Table 1**. We then performed RNA sequencing on these samples and applied the LENS computational workflow (**Figure 1**). LENS is an open-source method that predicts tumor-specific and tumor-associated antigens from genomic data (27). LENS predicted HLA Class I ligand binding in several CTAs but across multiple samples, only PRAME and NUTM1 reliably had predicted epitopes. Interestingly, LENS predicted the translationally relevant $PRAME_{425\text{-}433}$ SLLQHLIGL epitope in every sample except for TC-797 in which *PRAME* was transcriptionally silent (28, 29). Whole genome long-read DNA sequencing failed to identify a genetic cause for the absence of PRAME expression in TC-797 (data not shown). In screening cancer/testis genes using our manually curated list of CTAs (**Supplementary Methods Table 3**), out of 164 different cancer/testis genes only *PRAME* was consistently expressed across the tested samples. We concluded that in this N=6 set of NUT carcinomas, PRAME and NUTM1 are the most promising sources of cancer-specific antigens for therapeutic action.

RNA sequencing and immunohistochemistry identify high frequency and levels of PRAME RNA and protein in NUT carcinoma patient samples

To determine if the predominance of *PRAME* and *NUTM1* expression among cancer/testis genes was reflected in patient samples, we searched the de-identified Tempus multimodal database for patients with detected *NUTM1* fusion genes (identified

via Tempus xT [solid-tumor DNA] (30), Tempus xR [solid-tumor RNA] (31), or Tempus xF [circulating tumor DNA] assays) (32). Research filters below clinical reporting were applied to obtain patients with evidence of a *NUTM1* fusion, defined as containing at least 10 total supporting reads from DNA or at least 5 total supporting reads from RNA. Subject to these thresholds, 165 patients had evidence of *NUTM1* fusions, with a total of 33 distinct fusion partners (**Table 2**). Consistent with their role as canonical NUT carcinoma fusion partners, *BRD4::NUTM1, NSD3::NUTM1,* and *BRD3::NUTM1* accounted for the majority of cases (35.8%, 17.6%, and 10.9% respectively) with the remaining samples harboring one of the 30 other fusion partners (**Supplementary Figure 1A).** As expected, *BRD4::NUTM1*, *BRD3::NUTM1*, and *NSD3::NUTM1* fusions primarily occurred in the lung and head/neck primary sites – typical anatomic locations for NUT carcinoma (9). Analysis of gene expression from 162 of the patients with available RNA data revealed that out of 157 CTA genes covered in the Tempus xR assay, *PRAME* was identified as having the highest average expression after *NUTM1* (**Figure 2A**). We observed a bimodal distribution of *PRAME* expression in comparison to *NUTM1* across the cohort, designating *PRAME*^{high} and *PRAME*^{low} groups using a threshold of 3.1 $\log_2$(TPM+1) (**Figure 2B**). We found the *BRD4::NUTM1* group to be significantly enriched in *PRAME*^{high} samples (fisher exact, p<0.001) with *BRD3::NUTM1* and *NSD3::NUTM1* also having more *PRAME*^{high} samples than *PRAME*^{low} (**Figure 2C**). Of the remaining non-canonical fusion partners, 14 partners had at least one instance of *PRAME*^{high} with 3 fusion partners having more than one: *MGA::NUTM1*, *SLC12A6::NUTM1*, and *CIC::NUTM1* (**Supplementary Figure 1B**). Notably, only 1 of 13 *YAP1::NUTM1* samples was classified as *PRAME*^{high}. Using the *PRAME*^{high} and

PRAME^{low} groups, we identified several primary sites with the highest percentage of *PRAME*^{high} samples (**Figure 2D**). These sites included multiple sinus regions, unspecified peripheral nervous system (PNS), thymus, trachea, liver, and vulva; most lung and head, face, or neck primary sites demonstrated high *PRAME* expression. To assess for protein level PRAME expression in NUT carcinoma patient samples, we also stained a previously described NUT carcinoma tissue microarray for PRAME and found PRAME staining in 43/77 (56%) of samples (**Figure 2E**) (33). We concluded that most NUT carcinomas transcribe and subsequently translate *PRAME* at levels and frequencies greater than other tested cancer/testis genes.

BRD4::NUTM1 drives PRAME expression

Due to the high levels and frequency of *PRAME* observed in cell lines (N=5), a patient derived xenograft (N=1), the Tempus AI sequencing database (N=165), and the NUT carcinoma tissue microarray (N=77), and because PRAME expression is regulated by epigenetic changes including H3K27 acetylation in non-malignant human physiology (34), we hypothesized that *NUTM1* fusion oncoproteins might be contributing to transcriptional dysregulation and causing the ectopic expression of PRAME. To test this hypothesis, we transduced HEK 293T cells with tet-on *BRD4::NUTM1* or *eGFP* lentiviral particles and observed an increase in PRAME protein levels with *BRD4::NUTM1* expression but not with GFP (**Figure 3A**). We then used siRNAs targeting *NUTM1* to knockdown BRD4::NUTM1 in the five NUT carcinoma cell lines and immunoblotted for PRAME (**Figure 3B**). We found that in all cell lines except for the *PRAME* negative TC-797 cell line, BRD4::NUTM1 loss was accompanied by a decrease in PRAME protein

levels. The decrease in PRAME with BRD4::NUTM1 knockdown was marginal in 14169 compared to other NUT carcinoma cell lines, so we performed a western blot time course in 14169 cells which revealed a greater effect on PRAME levels at a later timepoint, 4 days instead of 3 days, after *NUTM1* siRNA transfection (**Figure 3C**). We considered whether these effects might be mediated through the corresponding loss of MYC after BRD4::NUTM1 knockout, but our review of the thorough literature identifying MYC-target genes we could find no evidence to suggest that *PRAME* is a MYC-target gene. We concluded that BRD4::NUTM1 is contributing to the expression of PRAME in *BRD4::NUTM1* NUT carcinomas, probably independent of MYC.

Immunopeptidomics on NUT carcinoma samples identifies more HLA Class I PRAME ligands than all other analyzed CTAs combined

We hypothesized that if cytosolic PRAME levels are high in NUT carcinoma, then HLA Class I-bound PRAME epitopes would be detectable using untargeted mass spectrometry/immunopeptidomics. Untargeted mass spectrometry was performed with the five cell lines and with the PDX to identify and characterize NUTM1, PRAME, and other CTA epitopes being presented by HLA Class I molecules and to guide therapeutic TCR selection. We identified a total of 33,644 unique peptides, 159 of which were shared by all samples **(Supplementary Figure 2**). Focusing on the presented CTAs, we identified 14 unique peptides from 6 proteins out of all CTAs with detection in at least 1 sample. Of these 14 peptides, 9 corresponded to PRAME and 1 corresponded to NUTM1 (**Figure 4A**). The remaining four CTA peptides corresponded to KKCL1, MAGA1, CTGE2, and ACTL8. As expected, the *PRAME* negative TC-797 revealed no

PRAME epitopes. The well described $PRAME_{425}$ SLLQHLIGL epitope was detected in the HLA A02+ PER-403 and PDX samples (**Figure 4B**) (35-37). To detect fusion junctional peptides, long read RNA sequencing was performed and used to generate consensus fusion sequences (**Supplementary Figure 3**). The reference human proteome was augmented with these fusion sequences for peptide mapping, but no junctional fusion peptides were detected. Based on the increased prevalence of PRAME epitopes in our samples relative to NUTM1 and based on the availability of existing PRAME therapeutics for testing, we hypothesized PRAME epitopes are more likely to be imminently actionable than NUTM1 epitopes in NUT carcinoma.

PRAME+ but not PRAME- NUT carcinoma cells are susceptible to T-cell killing mediated by an $\alpha PRAME_{425}$ x SP34 αCD3 bispecific molecule

Whether NUT carcinoma is susceptible to TCR-mediated therapeutics like TCR bispecifics or TCR T-cell therapies is unknown. To explore this issue and to evaluate the translational relevance of PRAME cancer-specific antigens, we created an $\alpha PRAME_{425}$ TCR x SP34 αCD3 BiTE molecule with the same variable regions as the affinity-matured TCR BiTE IMC-F106C (**Figure 5A**). IMC-F106C has been through phase I/II testing and is currently being evaluated as first line therapy in a randomized phase 3 trial (NCT06112314) for melanoma patients (38). Because our $\alpha PRAME_{425}$ TCR x SP34 αCD3 BiTE has significant homology to IMC-F106C including perfect homology to the variable regions of the TCR, we anticipated our bispecific molecule to have specificity for the same $PRAME_{425}$ SLLQHLIGL epitope IMC-F106C targets. We used SLLQHLIGL

peptide pulsing and TAP deficient T2 cells in co-culture with allogeneic T-cells to demonstrate enhancement of bispecific-mediated cytotoxicity with peptide pulse. TAP deficient T2 cells have empty HLA molecules on the cell surface and are loaded by incubating the cells in the presence of peptide ligands that will bind HLA. Killing of peptide-pulsed T2 cells thus demonstrated the specificity of the bispecific molecule for the SLLQHLIGL epitope (**Figure 5B**). We then titrated the concentration of the bispecific in the co-cultures of a *PRAME*+, HLA A02+ NSCLC cell line in the presence of allogeneic T-cells and found a dose-dependent effect (**Figure 5C**). The *PRAME* negative TC-797 and the *PRAME* positive 10-15 and 14169 cell lines were tested alongside a haplo-incompatible NSCLC cell line (H460, HLA A*24:02, *68:01) for T-cell mediated cytotoxicity in co-culture experiments using 10^{-8} M of bispecific molecule. We observed no cytotoxic effect of the bispecific in TC-797 or H460 at either of the tested effector: target ratios but we did observe potent cytotoxicity that was enhanced by a higher effector:target ratio in both *PRAME* positive NUT carcinoma cell lines (**Figure 5D**). Interestingly, the SLLQHLIGL epitope was predicted by LENS in 10-15 and 14169 but not detected using untargeted mass spectrometry likely due to the limited sensitivity of immunopeptidomics (39-41). We concluded that PRAME epitopes like SLLQHLIGL are a previously unappreciated therapeutic vulnerability in NUT carcinoma.

Discussion/Conclusion (Words=766):

Recent advances in antigen-directed immunotherapy have resulted in a new generation of “targeted immunotherapies” that leverage cell surface protein or TCR/peptide/HLA binding interactions for tumor targeting and specificity. Approved agents in solid tumors

target either HLA-presented peptide epitopes such as gp100 in uveal melanoma, MAGEA4/NY-ESO-1 epitopes in synovial sarcoma/myxoid round cell liposarcoma, or surface targets such as DLL3 in small cell lung cancer (14, 15). To identify promising targeted immunotherapies for NUT carcinoma, a highly lethal and treatment-refractory malignancy, we performed RNA sequencing on a selection of NUT carcinoma samples and applied the results to the antigen prediction software LENS which predicted PRAME as a plentiful source of cancer-specific antigens in NUT carcinoma and a dearth of other actionable CTAs (27). We found that *PRAME* was highly expressed in cell lines and the PDX model, consistent with observations in a large cohort of *NUTM1* fusion patient samples (especially among canonical *NUTM1* fusion patient samples) as well as in a NUT carcinoma tissue microarray.

Using genetic approaches, we further showed that elevated PRAME levels in *BRD4::NUTM1* NUT carcinoma are enhanced or at least maintained by BRD4::NUTM1. By applying immunopeptidomics to our panel of NUT carcinoma samples we also confirmed 9 PRAME epitopes, including the actionable SLLQHLIGL that is targeted by the clinically-tested IMC-F106C. NUTM1 epitopes were nearly absent from our immunopeptidomics results, likely due to immunoselection for non-antigenic fusion proteins, limitations of detection by shotgun immunopeptidomics, and/or strong nuclear localization of NUTM1 fusion proteins (13). PRAME epitopes are appealing candidates for peptide-HLA-directed therapeutics because of the strong localization of PRAME to the testis in healthy human physiology and because they arise as a direct result of the initiating genetic lesion in NUT carcinoma (*BRD4::NUTM1*). We created an αPRAME$_{425}$

TCR x SP34 αCD3 molecule that then showed potent, T-cell-mediated cytotoxicity against *PRAME*+ NUT carcinoma cells but not *PRAME*- NUT carcinoma cells. In total we showed here that the most common oncogene initiating NUT carcinoma, *BRD4::NUTM1*, enhances PRAME expression, that *PRAME* is a frequently and highly expressed cancer/testis gene in *BRD4::NUTM1, NSD3::NUTM1* and *BRD3::NUTM1* NUT carcinoma, and that the resulting PRAME epitopes are actionable targets for TCR therapeutics in NUT carcinoma.

Our work adds NUT carcinoma to the growing cadre of malignancies for which there is immense interest in targeting PRAME. Specifically, PRAME prevalence is high in genetically heterogeneous cancers including melanoma, acute myeloid leukemia, NSCLC, ovarian cancer, and others (42). In healthy human physiology, *PRAME* is turned on at the earliest stages of spermatogenesis and is silenced by histone modifications upstream of the translation initiation site (34). In malignancies, PRAME expression has been associated with worse clinical outcomes, DNA double strand breaks, aneuploidy, and genetic instability (34, 43-45). Oncogenic selection pressures in NUT carcinoma likely favor overriding the natural protections against ectopic PRAME production via BRD4::NUTM1-p300 acetylation of H3K27 (2, 33, 46). EZH2 is active in NUT carcinoma and promotes inhibitory trimethylation of H3K27 which is mutually exclusive with H3K27ac domains in NUT carcinoma (33). Thus, H3K27 trimethylation is a plausible mechanism by which TC-797 and other *BRD4::NUTM1* patient samples could restrict *PRAME* expression. Ultimately, further assays of histone states, such as ChIP-Seq or CUT&RUN, could explore this possibility. The mechanisms promoting

transcription of *PRAME* are likely conserved between BRD4::NUTM1, BRD3::NUTM1, and NSD3::NUTM1 because BRD4 and BRD3 are highly homologous (>80%) and because NSD3::NUTM1 recruits BRD4, thus forming a protein complex with the same constituents as BRD4::NUTM1 (19, 47).

A blossoming array of PRAME targeting TCR therapeutics including TCR T-cell therapies, endogenous T-cell therapy, TCR BiTEs/ImmTACs, tumor vaccines, and/or immunoglobulins specific for HLA-bound PRAME epitopes (“TCR mimetics”) may prove clinically effective in this challenging cancer. These agents include IMC-F106C, the second TCR bispecific (“ImmTAC”) in clinical testing (28, 29). A PRAME-specific TCR is included in the presently recruiting trial NCT05973487: a personalized TCR T-cell trial for patients with locally advanced or metastatic solid tumors. An RNA-loaded dendritic cell vaccine using *PRAME* has completed phase I testing for allogeneic stem cell transplant-ineligible acute myeloid leukemia and other PRAME vaccines are in development (48, 49). Pr20, a PRAME-specific TCR mimetic has been developed and showed activity against human leukemias in xenografts (50).

This growing set of PRAME therapeutics may have greater efficacy in NUT carcinoma than in NSCLC or other common malignancies without unifying genetic etiologies because of a mechanistic link between the central genetic rearrangements in NUT carcinoma and *PRAME* expression. Clinical trials testing PRAME therapeutics like IMC-F106C, Pr20, PRAME vaccines, or PRAME TCR T-cells in NUT carcinoma are a logical

next step especially given the moral imperative of discovering efficacious treatments for this rare, orphan disease patient population.

References:

1. Eagen KP, French CA. Supercharging BRD4 with NUT in carcinoma. Oncogene. 2021;40(8):1396–408.
2. Alekseyenko AA, Walsh EM, Wang X, Grayson AR, Hsi PT, Kharchenko PV, et al. The oncogenic BRD4-NUT chromatin regulator drives aberrant transcription within large topological domains. Genes & Development. 2015;29(14):1507–23.
3. Wang R, Liu W, Helfer CM, Bradner JE, Hornick JL, Janicki SM, et al. Activation of SOX2 expression by BRD4-NUT oncogenic fusion drives neoplastic transformation in NUT midline carcinoma. Cancer research. 2014;74(12):3332–43.
4. Kloker LD, Sidiras M, Flaadt T, Brecht IB, Deinzer CKW, Groß T, et al. Clinical management of NUT carcinoma (NC) in Germany: Analysis of survival, therapy response, tumor markers and tumor genome sequencing in 35 adult patients. Lung Cancer. 2024;189:107496.
5. Flaadt T, Wild H, Abele M, Frühwald M, Dirksen U, Classen CF, et al. NUT carcinoma in pediatric patients: Characteristics, therapeutic regimens, and outcomes of 11 cases registered with the German Registry for Rare Pediatric Tumors (STEP). Pediatric Blood & Cancer. 2024;71(3):e30821.
6. Lemelle L, Moya-Plana A, Dumont B, Fresneau B, Laprie A, Claude L, et al. NUT carcinoma in children, adolescents and young adults. Bulletin du Cancer. 2022;109(4):491–504.
7. French CA. Pathogenesis of NUT Midline Carcinoma. Annual Review of Pathology: Mechanisms of Disease. 2012;7(1):247–65.
8. Bauer DE, Mitchell CM, Strait KM, Lathan CS, Stelow EB, Lüer SC, et al. Clinicopathologic Features and Long-term Outcomes of NUT Midline Carcinoma. Clinical Cancer Research. 2012;18(20):5773–9.
9. French CA, Cheng ML, Hanna GJ, DuBois SG, Chau NG, Hann CL, et al. Report of the first international symposium on NUT carcinoma. Clinical Cancer Research. 2022;28(12):2493–505.
10. Lewin J, Soria JC, Stathis A, Delord JP, Peters S, Awada A, et al. Phase Ib Trial With Birabresib, a Small-Molecule Inhibitor of Bromodomain and Extraterminal Proteins, in Patients With Selected Advanced Solid Tumors. J Clin Oncol. 2018;36(30):3007–14.
11. Piha-Paul SA, Hann CL, French CA, Cousin S, Braña I, Cassier PA, et al. Phase 1 study of molibresib (GSK525762), a bromodomain and extra-terminal domain protein inhibitor, in NUT carcinoma and other solid tumors. JNCI Cancer Spectrum. 2020;4(2):pkz093.
12. Shapiro GI, LoRusso P, Dowlati A, T. Do K, Jacobson CA, Vaishampayan U, et al. A Phase 1 study of RO6870810, a novel bromodomain and extra-terminal protein inhibitor, in patients with NUT carcinoma, other solid tumours, or diffuse large B-cell lymphoma. British journal of cancer. 2021;124(4):744–53.
13. French CA, Ramirez CL, Kolmakova J, Hickman TT, Cameron MJ, Thyne ME, et al. BRD–NUT oncoproteins: a family of closely related nuclear proteins that block epithelial differentiation and maintain the growth of carcinoma cells. Oncogene. 2008;27(15):2237–42.

14. Nathan P, Hassel JC, Rutkowski P, Baurain J-F, Butler MO, Schlaak M, et al. Overall Survival Benefit with Tebentafusp in Metastatic Uveal Melanoma. New England Journal of Medicine. 2021;385(13):1196–206.
15. D'Angelo SP, Araujo DM, Abdul Razak AR, Agulnik M, Attia S, Blay J-Y, et al. Afamitresgene autoleucel for advanced synovial sarcoma and myxoid round cell liposarcoma (SPEARHEAD-1): an international, open-label, phase 2 trial. The Lancet. 2024;403(10435):1460–71.
16. D'Angelo SP, Furness AJS, Thistlethwaite F, Burgess MA, Riedel RF, Haanen J, et al. Lete-cel in patients with synovial sarcoma or myxoid/round cell liposarcoma: Planned interim analysis of the pivotal IGNYTE-ESO trial. American Society of Clinical Oncology; 2024.
17. Gazendam AM, Popovic S, Munir S, Parasu N, Wilson D, Ghert M. Synovial Sarcoma: A Clinical Review. Current Oncology. 2021;28(3):1909–20.
18. Knight JC, Renwick PJ, Dal Cin P, Van Den Berghe H, Fletcher CDM. Translocation t(12;16)(q13;p11) in Myxoid Liposarcoma and Round Cell Liposarcoma: Molecular and Cytogenetic Analysis1. Cancer Research. 1995;55(1):24–7.
19. Luo J, Bishop JA, DuBois SG, Hanna GJ, Sholl LM, Stelow EB, et al. Hiding in plain sight: NUT carcinoma is an unrecognized subtype of squamous cell carcinoma of the lungs and head and neck. Nature Reviews Clinical Oncology. 2025.
20. Durall RT, Huang J, Wojenski L, Huang Y, Gokhale PC, Leeper BA, et al. The BRD4–NUT Fusion Alone Drives Malignant Transformation of NUT Carcinoma. Cancer Research. 2023;83(23):3846–60.
21. Addis Philip W, Bedke Nicole JOY, Bouard L, Harper S, Liddy N, Mahon T, et al., inventors; IMMUNOCORE LTD, assignee. T CELL RECEPTORS. WO patent WO 2018/234319 A1. 2018 2018/06/19.
22. Froning K, Maguire J, Sereno A, Huang F, Chang S, Weichert K, et al. Computational stabilization of T cell receptors allows pairing with antibodies to form bispecifics. Nature Communications. 2020;11(1):2330.
23. Wu X, Sereno AJ, Huang F, Lewis SM, Lieu RL, Weldon C, et al., editors. Fab-based bispecific antibody formats with robust biophysical properties and biological activity. MAbs; 2015: Taylor & Francis.
24. Kudlacek ST, Metz S, Thiono D, Payne AM, Phan TT, Tian S, et al. Designed, highly expressing, thermostable dengue virus 2 envelope protein dimers elicit quaternary epitope antibodies. Science advances. 2021;7(42):eabg4084.
25. Bruderer R, Bernhardt OM, Gandhi T, Xuan Y, Sondermann J, Schmidt M, et al. Optimization of Experimental Parameters in Data-Independent Mass Spectrometry Significantly Increases Depth and Reproducibility of Results *. Molecular & Cellular Proteomics. 2017;16(12):2296–309.
26. Tognetti M, Sklodowski K, Müller S, Kamber D, Muntel J, Bruderer R, et al. Biomarker Candidates for Tumors Identified from Deep-Profiled Plasma Stem Predominantly from the Low Abundant Area. Journal of Proteome Research. 2022;21(7):1718–35.
27. Vensko SP, Olsen K, Bortone D, Smith CC, Chai S, Beckabir W, et al. LENS: Landscape of Effective Neoantigens Software. Bioinformatics. 2023;39(6):btad322.
28. Davar D, Williams A, Lopez J, Olson D, Sato T, Shaw H, et al. 694 Phase 1 safety and efficacy of brenetafusp, a PRAME × CD3 ImmTAC bispecific, in post-

checkpoint cutaneous melanoma (CM). Journal for ImmunoTherapy of Cancer. 2024;12(Suppl 2):A796–A.

29. Friedman C, De Burgh Williams A, Lopez JS, Ouali K, Middleton MR, Thistlethwaite F, et al. 750P Phase I safety and efficacy of brenetafusp, a PRAME × CD3 ImmTAC T cell engager, in platinum resistant ovarian cancer (PROC). Annals of Oncology. 2024;35:S569–S70.

30. Beaubier N, Tell R, Lau D, Parsons JR, Bush S, Perera J, et al. Clinical validation of the tempus xT next-generation targeted oncology sequencing assay. Oncotarget. 2019;10(24):2384–96.

31. Michuda J, Breschi A, Kapilivsky J, Manghnani K, McCarter C, Hockenberry AJ, et al. Validation of a Transcriptome-Based Assay for Classifying Cancers of Unknown Primary Origin. Mol Diagn Ther. 2023;27(4):499–511.

32. Finkle JD, Boulos H, Driessen TM, Lo C, Blidner RA, Hafez A, et al. Validation of a liquid biopsy assay with molecular and clinical profiling of circulating tumor DNA. NPJ Precis Oncol. 2021;5(1):63.

33. Huang Y, Durall RT, Luong NM, Hertzler HJ, Huang J, Gokhale PC, et al. EZH2 cooperates with BRD4-NUT to drive NUT carcinoma growth by silencing key tumor suppressor genes. Cancer research. 2023;83(23):3956–73.

34. Kurtenbach S, Sanchez MI, Kuznetsoff J, Rodriguez DA, Weich N, Dollar JJ, et al. PRAME induces genomic instability in uveal melanoma. Oncogene. 2024;43(8):555–65.

35. Spel L, Boelens JJ, van der Steen DM, Blokland NJ, van Noesel MM, Molenaar JJ, et al. Natural killer cells facilitate PRAME-specific T-cell reactivity against neuroblastoma. Oncotarget. 2015;6(34):35770–81.

36. Rosskopf S, Leitner J, Paster W, Morton LT, Hagedoorn RS, Steinberger P, et al. A Jurkat 76 based triple parameter reporter system to evaluate TCR functions and adoptive T cell strategies. Oncotarget. 2018;9(25):17608–19.

37. Pentcheva-Hoang T, Torres D, Rodriguez T, Korngold A, Lu A, Crisostomo J, et al. Inducible MyD88/CD40 (iMC) Enhances Proliferation and Survival of Tumor-Specific TCR-Modified T Cells and Improves Anti-Tumor Efficacy in Myeloma. Blood. 2016;128(22):4550.

38. Hamid O, Sato T, Davar D, Callahan MK, Thistlethwaite F, Aljumaily R, et al. 728O Results from phase I dose escalation of IMC-F106C, the first PRAME × CD3 ImmTAC bispecific protein in solid tumors. Annals of Oncology. 2022;33:S875.

39. Wilhelm M, Zolg DP, Graber M, Gessulat S, Schmidt T, Schnatbaum K, et al. Deep learning boosts sensitivity of mass spectrometry-based immunopeptidomics. Nature Communications. 2021;12(1):3346.

40. C. Silva AS, Bouwmeester R, Martens L, Degroeve S. Accurate peptide fragmentation predictions allow data driven approaches to replace and improve upon proteomics search engine scoring functions. Bioinformatics. 2019;35(24):5243–8.

41. Li K, Jain A, Malovannaya A, Wen B, Zhang B. DeepRescore: Leveraging Deep Learning to Improve Peptide Identification in Immunopeptidomics. PROTEOMICS. 2020;20(21-22):1900334.

42. Al-Khadairi G, Decock J. Cancer Testis Antigens and Immunotherapy: Where Do We Stand in the Targeting of PRAME? Cancers. 2019;11(7):984.

43. Doolan P, Clynes M, Kennedy S, Mehta JP, Crown J, O'Driscoll L. Prevalence and prognostic and predictive relevance of PRAME in breast cancer. Breast Cancer Research and Treatment. 2008;109(2):359–65.
44. Epping MT, Hart AAM, Glas AM, Krijgsman O, Bernards R. PRAME expression and clinical outcome of breast cancer. British Journal of Cancer. 2008;99(3):398–403.
45. Takata K, Chong LC, Ennishi D, Aoki T, Li MY, Thakur A, et al. Tumor-associated antigen PRAME exhibits dualistic functions that are targetable in diffuse large B cell lymphoma. The Journal of Clinical Investigation. 2022;132(10).
46. Alekseyenko AA, Walsh EM, Zee BM, Pakozdi T, Hsi P, Lemieux ME, et al. Ectopic protein interactions within BRD4–chromatin complexes drive oncogenic megadomain formation in NUT midline carcinoma. Proceedings of the National Academy of Sciences. 2017;114(21):E4184–E92.
47. Rahman S, Sowa ME, Ottinger M, Smith JA, Shi Y, Harper JW, et al. The Brd4 extraterminal domain confers transcription activation independent of pTEFb by recruiting multiple proteins, including NSD3. Mol Cell Biol. 2011;31(13):2641–52.
48. Fløisand Y, Remberger M, Bigalke I, Josefsen D, Vålerhaugen H, Inderberg EM, et al. WT1 and PRAME RNA-loaded dendritic cell vaccine as maintenance therapy in de novo AML after intensive induction chemotherapy. Leukemia. 2023;37(9):1842–9.
49. Bayat Z, Majidi Z, Taherkhani A, Samie L. Engineering a Novel T-Cell Epitope-Based Vaccine Targeting PRAME in Cancer Immunotherapy. Peptide Science. 2025;117(1):e24393.
50. Chang AY, Dao T, Gejman RS, Jarvis CA, Scott A, Dubrovsky L, et al. A therapeutic T cell receptor mimic antibody targets tumor-associated PRAME peptide/HLA-I antigens. The Journal of Clinical Investigation. 2017;127(7):2705–18.

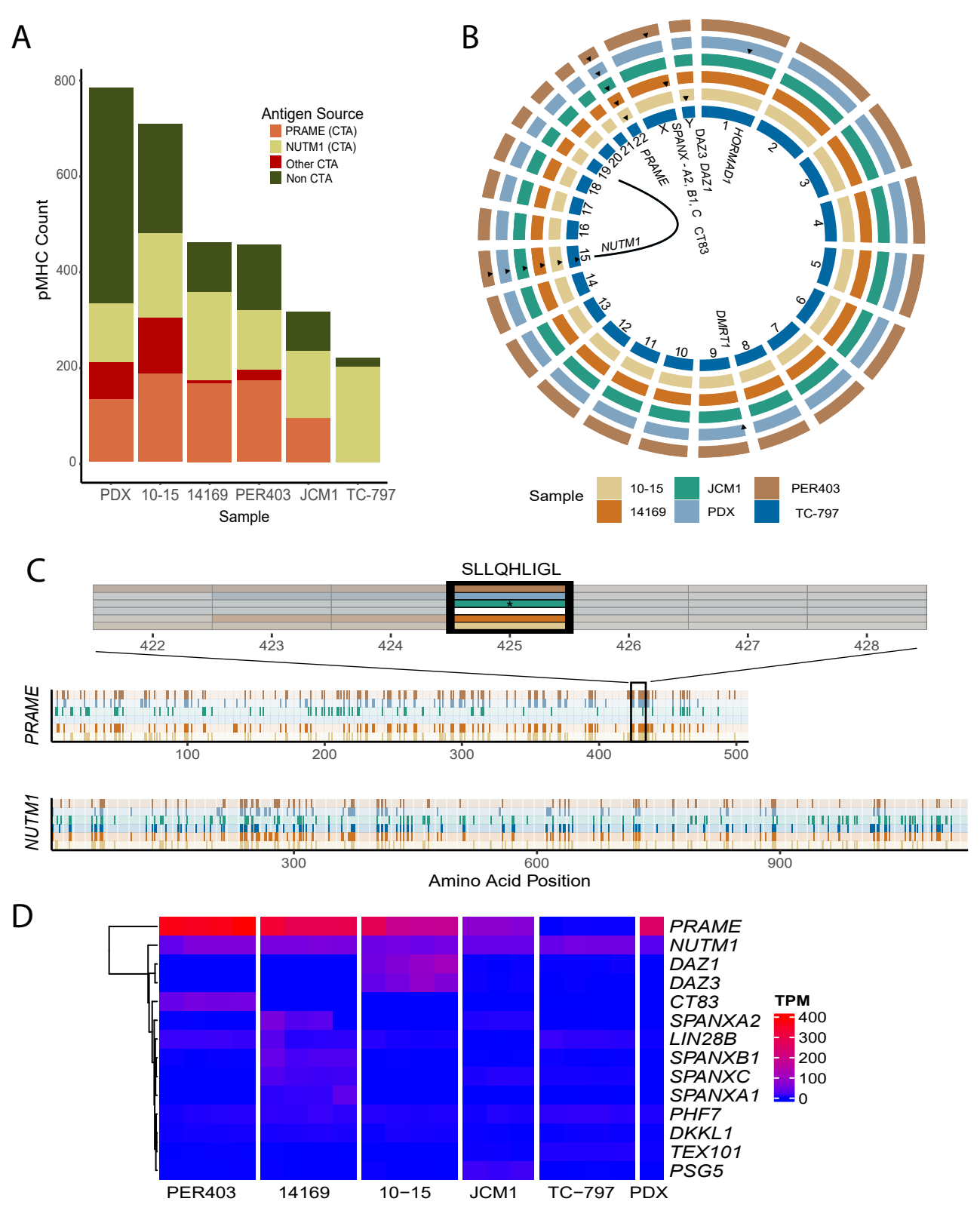
A
800
600
400
200
0
pMHC Count
Antigen Source
PRAME (CTA)
NUTM1 (CTA)
Other CTA
Non CTA
PDX
10-15
14169
PER403
JCM1
TC-797
Sample
B
HORMAD1
DAZ3 DAZ1
SPANX - A2, B1, C
CT83
DMRT1
PRAME
NUTM1
Sample
10-15
14169
JCM1
PDX
PER403
TC-797
C
SLLQHLIGL
422
423
424
425
426
427
428
PRAME
100
200
300
400
500
NUTM1
300
600
900
Amino Acid Position
D
PRAME
NUTM1
DAZ1
DAZ3
CT83
SPANXA2
LIN28B
SPANXB1
SPANXC
SPANXA1
PHF7
DKKL1
TEX101
PSG5
TPM
400
300
200
100
0
PER403
14169
10−15
JCM1
TC−797
PDX

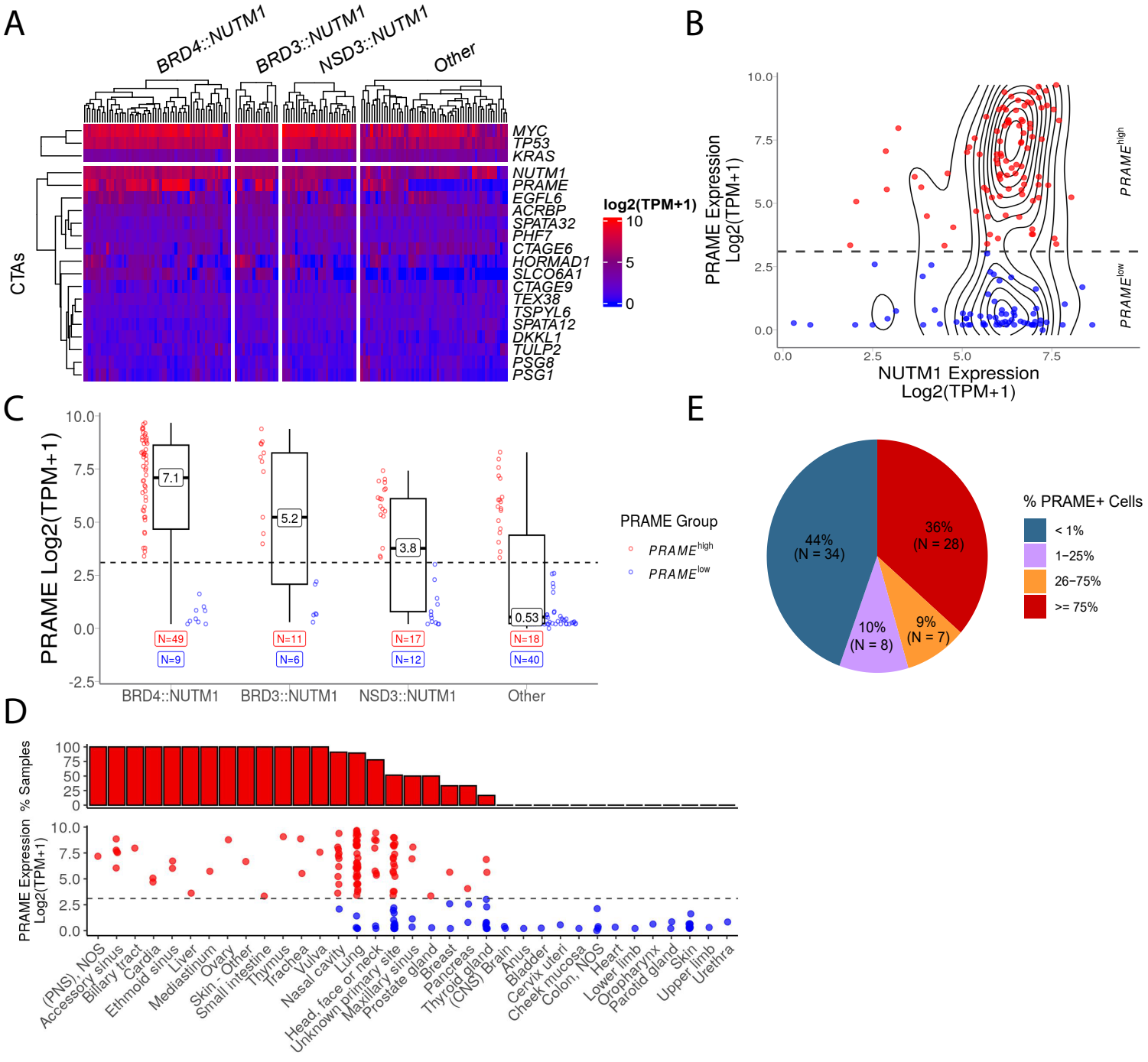
A
BRD4::NUTM1
BRD3::NUTM1
NSD3::NUTM1
Other
MYC
TP53
KRAS
NUTM1
PRAME
EGFL6
ACRBP
SPATA32
PHF7
CTAGE6
HORMAD1
SLCO6A1
CTAGE9
TEX38
TSPYL6
SPATA12
DKKL1
TULP2
PSG8
PSG1
CTAs
log2(TPM+1)
10
5
0
B
PRAME Expression Log2(TPM+1)
NUTM1 Expression Log2(TPM+1)
PRAME^high
PRAME^low
C
PRAME Log2(TPM+1)
7.1
5.2
3.8
0.53
N=49
N=9
N=11
N=6
N=17
N=12
N=18
N=40
BRD4::NUTM1
BRD3::NUTM1
NSD3::NUTM1
Other
PRAME Group
PRAME^high
PRAME^low
E
44% (N = 34)
36% (N = 28)
10% (N = 8)
9% (N = 7)
% PRAME+ Cells
< 1%
1–25%
26–75%
>= 75%
D
% Samples
PRAME Expression Log2(TPM+1)
(PNS), NOS
Accessory sinus
Biliary tract
Cardia
Ethmoid sinus
Liver
Mediastinum
Ovary
Skin - Other
Small intestine
Thymus
Trachea
Vulva
Nasal cavity
Lung
Head, face or neck
Unknown primary site
Maxillary sinus
Prostate gland
Breast
Pancreas
Thyroid gland
(CNS) Brain
Anus
Bladder
Cervix uteri
Cheek mucosa
Colon, NOS
Heart
Lower limb
Oropharynx
Parotid gland
Skin
Upper limb
Urethra

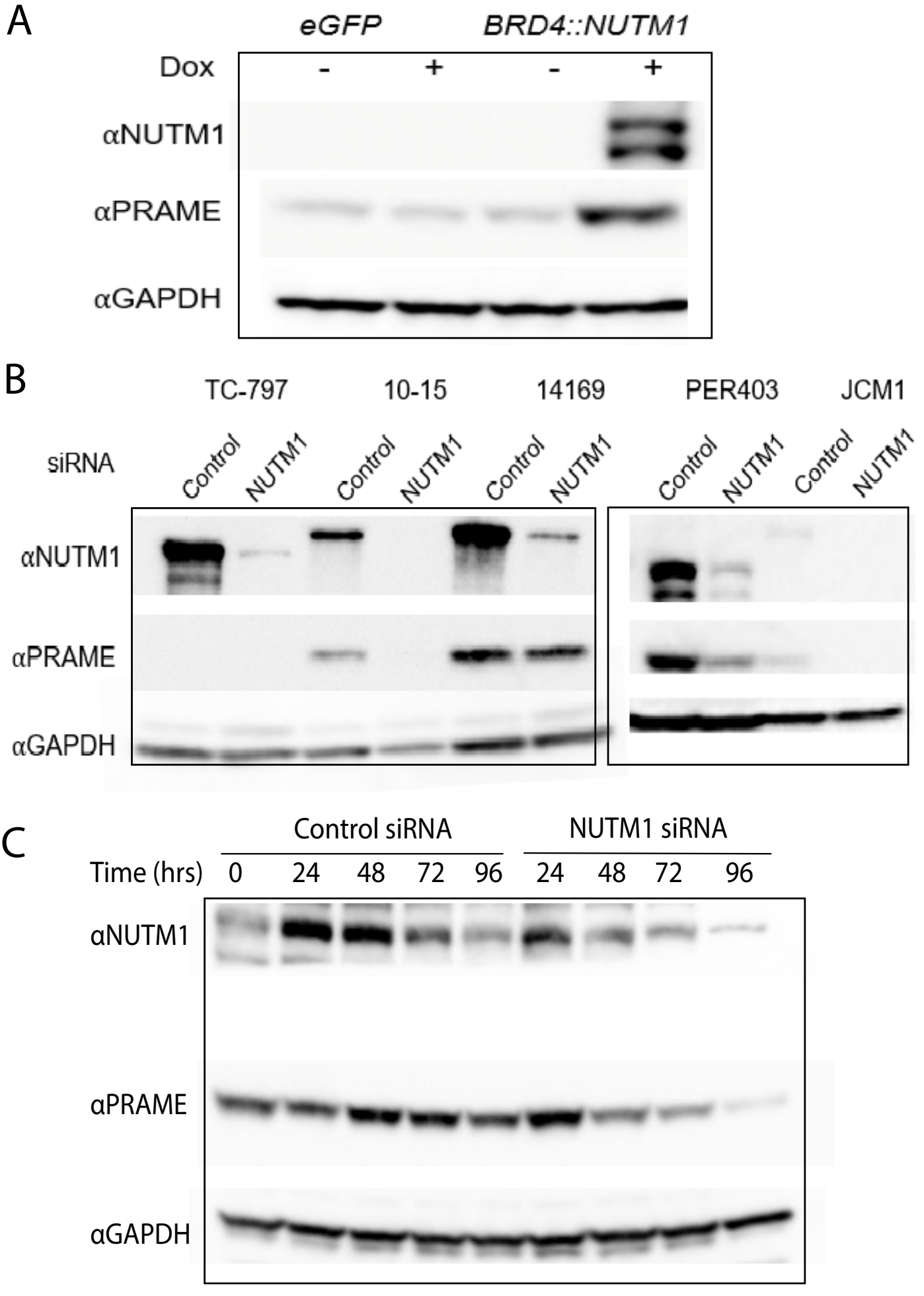
A
eGFP
BRD4::NUTM1
Dox
-
+
-
+
αNUTM1
αPRAME
αGAPDH
B
TC-797
10-15
14169
PER403
JCM1
siRNA
Control
NUTM1
Control
NUTM1
Control
NUTM1
Control
NUTM1
Control
NUTM1
αNUTM1
αPRAME
αGAPDH
C
Control siRNA
NUTM1 siRNA
Time (hrs)
0
24
48
72
96
24
48
72
96
αNUTM1
αPRAME
αGAPDH

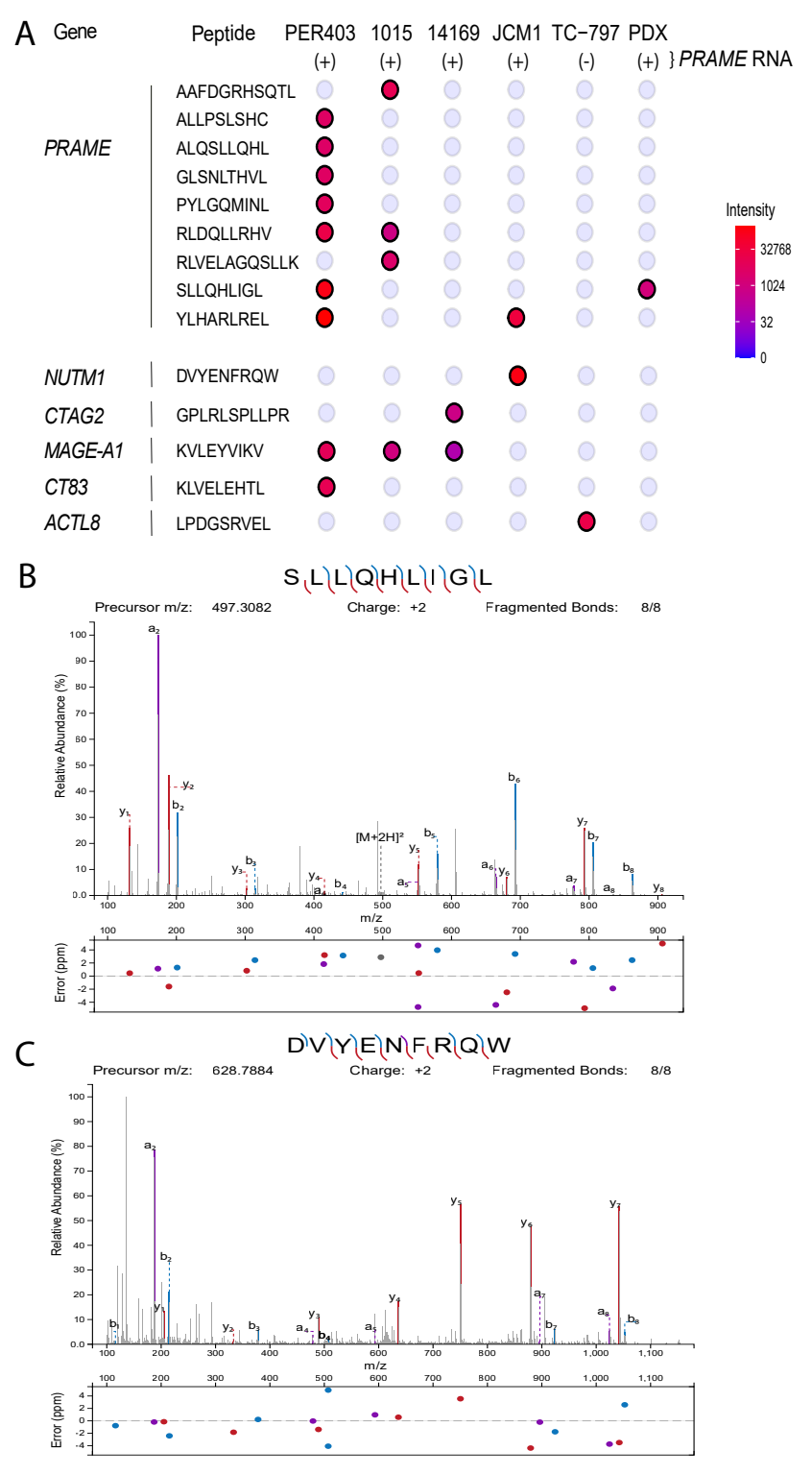
A
Gene
Peptide
PER403
1015
14169
JCM1
TC−797
PDX
(+)
(+)
(+)
(+)
(-)
(+)
PRAME RNA
PRAME
AAFDGRHSQTL
ALLPSLSHC
ALQSLLQHL
GLSNLTHVL
PYLGQMINL
RLDQLLRHV
RLVELAGQSLLK
SLLQHLIGL
YLHARLREL
NUTM1
DVYENFRQW
CTAG2
GPLRLSPLLPR
MAGE-A1
KVLEYVIKV
CT83
KLVELEHTL
ACTL8
LPDGSRVEL
Intensity
32768
1024
32
0
B
S L L Q H L I G L
Precursor m/z: 497.3082
Charge: +2
Fragmented Bonds: 8/8
Relative Abundance (%)
m/z
Error (ppm)
[M+2H]²
C
D V Y E N F R Q W
Precursor m/z: 628.7884
Charge: +2
Fragmented Bonds: 8/8
Relative Abundance (%)
m/z
Error (ppm)

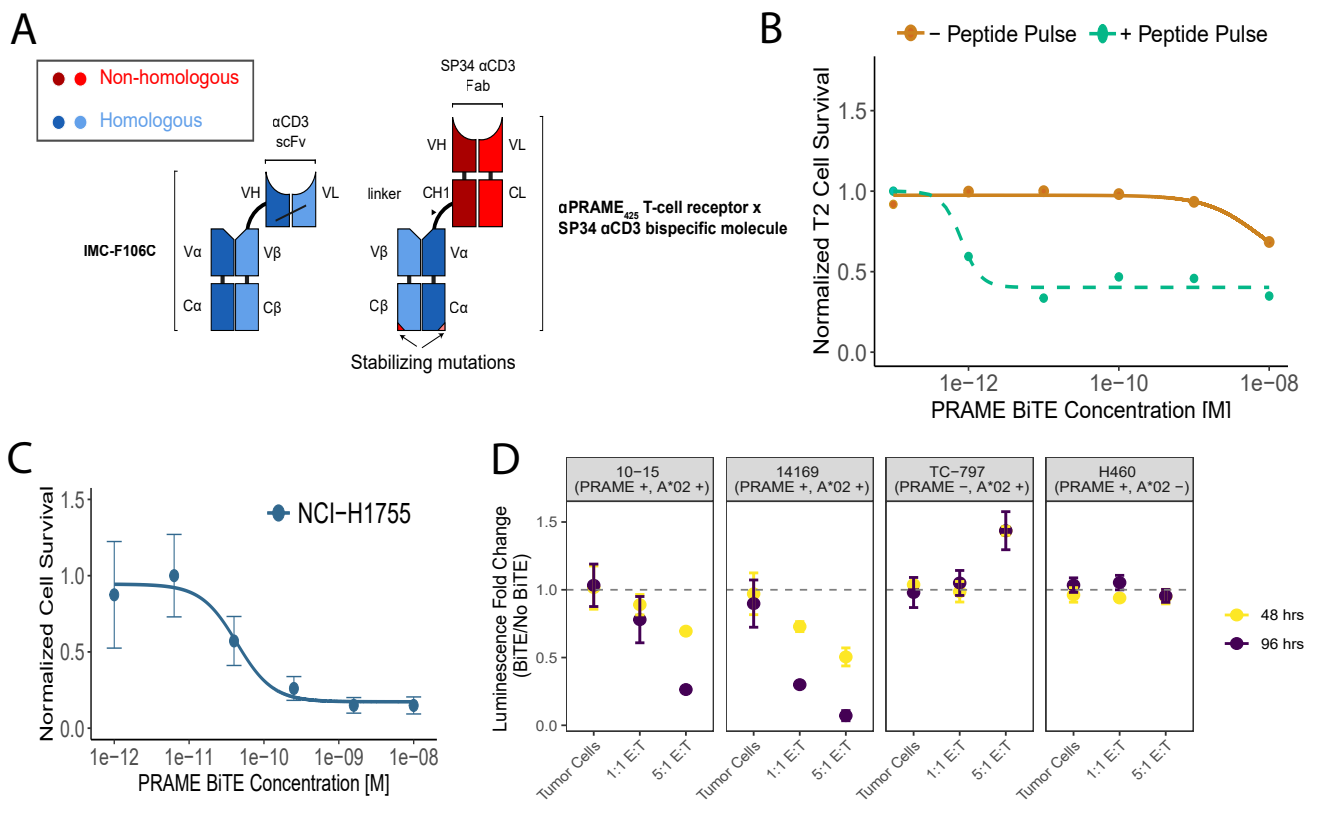
A
Non-homologous
Homologous
αCD3
scFv
VH
VL
IMC-F106C
Vα
Vβ
Cα
Cβ
SP34 αCD3
Fab
VH
VL
linker
CH1
CL
Vβ
Vα
Cβ
Cα
Stabilizing mutations
αPRAME425 T-cell receptor x
SP34 αCD3 bispecific molecule
B
− Peptide Pulse
+ Peptide Pulse
Normalized T2 Cell Survival
1.5
1.0
0.5
0.0
1e−12
1e−10
1e−08
PRAME BiTE Concentration [M]
C
NCI−H1755
Normalized Cell Survival
1.5
1.0
0.5
0.0
1e−12
1e−11
1e−10
1e−09
1e−08
PRAME BiTE Concentration [M]
D
10−15
(PRAME +, A*02 +)
14169
(PRAME +, A*02 +)
TC−797
(PRAME −, A*02 +)
H460
(PRAME +, A*02 −)
Luminescence Fold Change
(BiTE/No BiTE)
1.5
1.0
0.5
0.0
Tumor Cells
1:1 E:T
5:1 E:T
48 hrs
96 hrs